Journal of Catalysis 259 (2008) 36–42

Contents lists available at ScienceDirect

Journal of Catalysis

www.elsevier.com/locate/jcat

Evaluation of catalytic activity of Ga_2O_3–Al_2O_3 solid solutions for CH_4-SCR by UV–vis spectra after adsorption of C_3H_6 as a probe

Yuya Miyahara [a], Tsunenori Watanabe [a,b], Takeo Masuda [a], Hiroyoshi Kanai [a], Hiroshi Deguchi [b], Masashi Inoue [a,*]

[a] Department of Energy and Hydrocarbon Chemistry, Graduate School of Engineering, Kyoto University, Katsura, Kyoto 615-8510, Japan
[b] The Kansai Electric Power Company, Inc., 3-11-20 Nakoji, Amagasaki 661-0974, Japan

ARTICLE INFO

Article history:
Received 17 May 2008
Revised 10 July 2008
Accepted 11 July 2008
Available online 12 August 2008

Keywords:
Propylene
UV–vis spectrum
Surface structure
Selective catalytic reduction
NO

ABSTRACT

When γ-Ga_2O_3–Al_2O_3 solid solutions were treated with C_3H_6 followed by heating at 300 °C, they were colored yellow giving two bands at 340 nm (α band) and 430 nm (β band) in their UV–vis spectra. The α and β bands were closely related with surface tetrahedral (T_d)-Ga^{3+} and octahedral (O_h)-Ga^{3+} sites, respectively. The intensities of the two bands changed by γ-Ga_2O_3–Al_2O_3 solid solutions prepared by various methods, although they had almost the same proportions of T_d-Ga^{3+} sites in the bulk structure. The intensities of the two bands can be used to diagnose the catalytic activity of γ-Ga_2O_3–Al_2O_3 catalysts for CH_4-SCR of NO.

1. Introduction

Catalytic reduction of nitric oxide (NO) can be achieved by direct decomposition or selective catalytic reduction (SCR) [1]. Among the possible reductants for SCR of NO, methane is the cheapest and SCR of NO with CH_4 has attracted much attention as an innovative technology for abatement of NO_x from stationary sources where the NH_3-SCR process is now applied. So far, various kinds of catalysts, i.e., zeolites, metal oxides and noble metals, have been examined. Transition-metal ion-exchanged zeolite catalysts have activities for CH_4-SCR [2–4]. Indium- and Ga-exchanged zeolites also showed activities for the reaction [5,6]. Recently, non-zeolitic catalysts have been investigated for practical use. Shimizu et al. reported that γ-alumina-supported gallium oxide (Ga_2O_3/γ-Al_2O_3) catalysts prepared by impregnation of γ-Al_2O_3 with a gallium nitrate solution showed high activities for CH_4-SCR [7,8].

In our previous research, we showed that γ-Ga_2O_3–Al_2O_3 solid solutions prepared by the glycothermal method had high activities for CH_4-SCR [9,10]. Further improvement of the catalyst was attained by γ-Ga_2O_3–Al_2O_3 solid solutions prepared by the solvothermal method using diethylenetriamine as a solvent [11].

The active sites of the Ga_2O_3–Al_2O_3 system have been investigated in detail, and it was concluded that tetrahedral (T_d)-Ga^{3+} with octahedral (O_h)-Al^{3+} at the next-nearest-neighboring (NNN) sites was active for the CH_4-SCR reaction [10]. Shimizu et al. also reached a similar conclusion for alumina-supported Ga_2O_3 catalysts [8]. Haneda et al. reported that the synergistic effect of Ga^{3+} and Al^{3+} in Ga_2O_3–Al_2O_3 prepared by the sol–gel method was an important factor in the C_3H_6-SCR reaction [12]. Since Ga^{3+} ions preferentially occupy the T_d sites of the defect spinel structure, the Ga/(Ga + Al) ratio is the prime factor controlling the activity of the Ga_2O_3–Al_2O_3 solid solution prepared by the solvothermal method, and the solid solution with Ga/(Ga + Al) = 0.3 showed the highest activity.

Another important factor affecting the steady-state activity was the crystallite size of the solid solution, and the catalyst with larger crystallite size exhibited higher activity albeit with a lower surface area. Catalysts with various crystallite sizes were prepared by the choice of media used for the solvothermal synthesis of catalysts [13]. For the Ga_2O_3–Al_2O_3–ZnO spinel catalyst system, the catalyst with larger crystallite size also showed higher activity for CH_4-SCR. Because water is produced by the reaction of CH_4 with NO, these results were explained in terms of the inhibitory effect of adsorbed water [14]. The catalyst with smaller crystallite size adsorbs a larger amount of water and exhibits lower steady-state activity. However, the γ-Ga_2O_3–Al_2O_3 solid solutions with larger crystallite sizes did show higher NO conversion even at the initial stage of the SCR reaction, as shown in this paper. Since the catalyst surface can be considered free from adsorbed water at the initial stage of the reaction, we have to find the origin of the crystallite-size effect.

We have found an interesting phenomenon whereby γ-Ga_2O_3–Al_2O_3 solid solutions pretreated in O_2 turned yellow on heating up to 300 °C in a C_3H_6 atmosphere. The color density seemed to

* Corresponding author.
E-mail address: inoue@scl.kyoto-u.ac.jp (M. Inoue).

0021-9517/$ – see front matter
doi:10.1016/j.jcat.2008.07.007

be connected with the crystallite size, and we have therefore focused on the UV–vis spectra of C_3H_6-treated γ-Ga_2O_3–Al_2O_3 solid solutions. It was found that the UV–vis spectra were closely related with the surface structure of the catalyst and can therefore be used to diagnose catalytic activity.

2. Experimental

2.1. Preparation of catalysts

γ-Ga_2O_3–Al_2O_3 solid solutions were prepared by the solvothermal method [13]. In a typical synthesis, a mixture of gallium acetylacetonate and aluminum isopropoxide was suspended in 80 mL of a reaction medium (toluene (TOL), 1,4-diaminobutane (1,4DAB), diglycolamine (DGA), 2-methylaminoethanol (MAE), ethylene glycol (EG), 1,5-pentanediol (1,5PG), diethylenetriamine (dEtA), triethylenetetramine (tEtA), or tetraethylenepentamine (tEpA)) in a test tube, and it was placed in a 200-mL autoclave. In the gap between the autoclave wall and the test tube, an additional 30 mL of the reaction medium was placed. After the air in the autoclave was completely replaced with N_2, the reaction mixture was heated to 300 °C at a rate of 2.5 °C min^{-1}, kept at that temperature for 2 h, and then cooled to room temperature. The product was repeatedly washed with acetone by vigorous mixing and centrifuging and then air-dried. The solid solutions were calcined at 700 °C in air for 30 min.

A γ-Ga_2O_3–Al_2O_3 solid solution was also prepared by co-precipitation. To an aqueous nitrate mixture of $Ga(NO_3)_3{\cdot}nH_2O$ (Ga content = 18.9 wt%) and $Al(NO_3)_3{\cdot}9H_2O$ (200 mL, $[Ga^{3+}] + [Al^{3+}] = 0.2$ M), a 5 wt% aqueous ammonia solution was added dropwise until $[NH_4OH]/([Ga^{3+}] + [Al^{3+}]) = 1.5$ was achieved. The precipitate was washed with ion-exchanged water several times and then air-dried. The amorphous precursor was calcined at 700 °C for 30 min to give γ-Ga_2O_3–Al_2O_3.

The catalysts synthesized by the solvothermal method in various media and those obtained by co-precipitation are referred to as ST-solvent(x) and CP(x), respectively, where x stands for the Ga/(Ga + Al) charged ratio.

Reference mixed oxides, $MgGa_2O_4$ and $ZnGa_2O_4$, were prepared by the glycothermal method [15]. Magnesium acetylacetonate (zinc acetate) and gallium acetylacetonate ($M/(M + Ga) = 1/3$) used as the raw materials to synthesize $MgGa_2O_4$ ($ZnGa_2O_4$) were suspended in 1,4-butanediol, and the mixture was heated at 300 °C for 2 h. The as-synthesized products were calcined at 700 °C for 30 min.

2.2. Catalyst tests

Catalyst tests for the SCR of NO with methane were carried out in a fixed-bed flow reactor. The catalyst was pressed into pellets that were crushed into 10–22 mesh, and 0.50 g of the catalyst was set in the reactor. The catalyst bed was heated to 600 °C in a helium flow and held at that temperature for 30 min. Then, reaction gas composed of 1000 ppm NO, 1000 ppm CH_4, and 6.7% O_2 with helium balance was introduced to the catalyst bed at $W/F = 0.3$ g s mL^{-1} (SV ≈ 11,000 h^{-1}). The effluent gases from the reactor were periodically analyzed with an on-line gas chromatograph (CP2002 Chrompack) and the temperature of the reactor was gradually decreased at 50 °C intervals.

Initial activity for the SCR of NO with methane was also measured. Pretreatment conditions were the same as those described above (at 600 °C for 30 min in a helium flow). The catalyst bed was cooled to 400 °C in the helium gas flow and then reaction gas composed of 1000 ppm NO, 2000 ppm CH_4, 6.7% O_2, and helium balance (SV ≈ 11,000 h^{-1}) was introduced to the reactor. The effluent gases from the reactor were analyzed with the on-line gas chromatograph and the NO conversion at 10 min on stream was used as the initial activity of the catalyst.

2.3. UV–vis measurements

The UV–vis spectra were measured in situ in a quartz cell. The catalyst (0.3 g) was set in the quartz cell and evacuated at 200 °C. Then, 100 Torr of O_2 was introduced followed by heating the catalyst at 650 °C. After evacuation at 650 °C, 100 Torr of O_2 was introduced again and the cell was held at that temperature for 1 h. It was cooled to room temperature, and then O_2 was evacuated. After propylene (30 Torr) was introduced to the catalyst, the cell was heated to 300 °C and kept at that temperature for 15 min. Diffuse reflectance UV–vis spectroscopy was carried out with a JASCO V-650 spectrometer at room temperature. The UV–vis absorption spectrum of $BaSO_4$ packed in the quartz cell was used as the background, and spectra of the samples were obtained using the Kubelka–Munk function. The peak intensities were normalized in such a way that the absorbance of the O^{2-}-to-M^{3+} charge transfer band around 220 nm was adjusted to unity. The peak area of each band in the UV–vis spectra was estimated by fitting the Gauss function to the peak.

2.4. Characterization of the catalysts

Powder X-ray diffraction patterns were measured on a Shimadzu XD-D1 diffractometer using 30-kV, 900-W Cu$K\alpha$ radiation and a carbon monochromator. Crystallite size was calculated from the half-height width of the (440) diffraction peak of the spinel structure using the Scherrer equation.

The BET surface area was calculated using the single-point method based on nitrogen uptake measured at 77 K. The samples were pretreated in an N_2 flow at 300 °C for 30 min prior to measurement.

X-ray absorption fine structure (XAFS) measurements for the Ga K-edge were carried out on the BL16B2 beam line at SPring-8 (Harima). An Si(111) monochromator was used to monochromatize the X-ray. The absorption spectra in the energy range of the Ga K-edge were measured by transmission mode at room temperature. The proportions of T_d and O_h gallium sites in the samples were estimated by the linear combination fitting (LCF) method from their XANES data. γ-Ga_2O_3–Al_2O_3 with a Ga/(Ga + Al) ratio of 0.1 prepared solvothermally in MEA was used as the T_d standard sample, while $ZnGa_2O_4$ was applied for the O_h sample [16].

3. Results and discussion

3.1. Catalytic activities of Ga_2O_3–Al_2O_3 solid solutions

The characterized data of the Ga_2O_3–Al_2O_3 solid solutions obtained by various methods are summarized in Table 1. The γ-phase of Ga_2O_3–Al_2O_3 solid solutions having a defect spinel structure was obtained by most of the synthesis methods, and the BET surface areas of these catalysts ranged from 130 to 240 $m^2\,g^{-1}$. A significant difference among these catalysts is found in the crystallite size, which varied from amorphous (lower than the calculation limit) to 9.5 nm.

Fig. 1 shows the steady-state activities of the Ga_2O_3–Al_2O_3 catalysts with a Ga/(Ga + Al) charged ratio of 0.3. Although these catalysts contain the same amount of Ga^{3+} having the same crystal structure (except for ST-EG(0.3) which is amorphous), the catalyst activity varies widely. ST-MAE(0.3) has the largest BET surface area, but it shows relatively low activity. Moreover, ST-dEtA(0.3) which has a rather small surface area shows the highest activity. As described earlier, the catalytic activity for CH_4-SCR increases with an increase in the crystallite size [13].

Table 1
Physical properties of Ga_2O_3–Al_2O_3 solid solutions with a Ga/(Ga + Al) charged ratio of 0.3 prepared by solvothermal and co-precipitation methods

Reaction medium[a]	Crystal structure	Crystallite size (nm)	S_{BET} ($m^2\,g^{-1}$)	Ga/(Ga + Al) ratio determined by	
				XPS	ICP
dEtA	γ-Type	9.5	157	0.24	0.25
tEtA	γ-Type	7.4	156	0.29	0.25
1,5PG	γ-Type	5.3	188	0.30	0.26
tEpA	γ-Type	5.0	186	0.33	0.25
DGA	γ-Type	4.8	188	0.35	0.24
TOL	γ-Type	4.5	186	0.30	0.25
1,4DAB	γ-Type	4.3	174	0.34	0.27
MAE	γ-Type	3.9	241	0.33	0.25
CP	γ-Type	2.8	137	0.30	0.26
EG	Amorphous	–	154	0.29	0.23

[a] Abbreviations for the medium for the solvothermal method or preparation method: dEtA, diethylenetriamine; tEtA, triethylenetetramine; 1,5PG, 1,5-pentanediol; tEpA, tetraethylenepentamine; DGA, diglycolamine; TOL, toluene; 1,4DAB, 1,4-diaminobutane; MAE, 2-methylaminoethanol; CP, co-precipitation; EG, ethylene glycol.

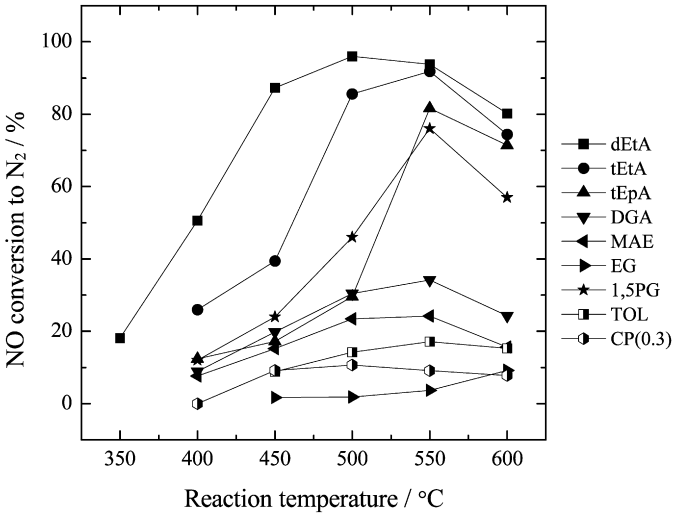

Fig. 1. Catalytic activity of the Ga_2O_3–Al_2O_3 solid solutions with a Ga/(Ga + Al) charged ratio of 0.3 prepared by the solvothermal and co-precipitation methods. Reaction conditions: NO 1000 ppm, CH_4 1000 ppm, O_2 6.7% and He balance. Abbreviations of solvents are shown in the footnote of Table 1.

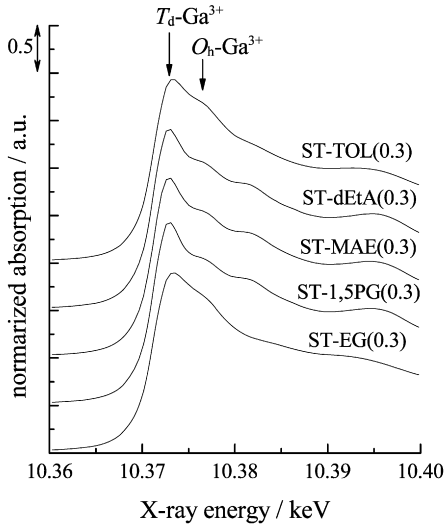

Fig. 2. Ga K-edge XANES spectra of Ga_2O_3–Al_2O_3 solid solutions prepared solvothermally in various media.

3.2. Local structure of Ga ions in Ga_2O_3–Al_2O_3 solid solutions

The Ga K-edge XANES spectra of the γ-Ga_2O_3–Al_2O_3 solid solutions are shown in Fig. 2. The absorption peak at 10.373 keV was assigned to the absorption of T_d-Ga^{3+}, and that at 10.376 keV, to the absorption of O_h-Ga^{3+} [8]. As shown in Fig. 2, the Ga K-edge XANES spectra were almost the same for the catalysts with a Ga/(Ga + Al) charged ratio of 0.3. However, the intensities of the O_h-Ga^{3+} absorption peaks of ST-EG(0.3) and ST-TOL(0.3) are slightly larger than those for the other catalysts.

Table 2
Linear combination fitting analysis of XANES spectra

Reaction medium	T_d-Ga^{3+} / (T_d-Ga^{3+} + O_h-Ga^{3+})	NO conversion at 500 °C (%)
Diethylenetriamine	0.84	96
1,5-Pentanediol	0.85	46
2-Methylaminoethanol	0.85	24
Toluene	0.71	14
Ethylene glycol	0.74	1.8

The ratios of T_d-Ga^{3+}/(T_d-Ga^{3+} + O_h-Ga^{3+}) were calculated by the LCF method on the basis of the spectra of the standard materials for T_d-Ga^{3+} and O_h-Ga^{3+}. The T_d-Ga^{3+} portions in Ga_2O_3–Al_2O_3 (Ga/(Ga + Al) = 0.3) ranged from 0.70 to 0.85 as shown in Table 2. This difference in the local structures of Ga^{3+} was too small to explain the large difference in the catalyst activities, and the catalytic activity for CH_4-SCR did not correlate with the proportion of T_d-Ga^{3+}. These results suggest that the local structure of surface Ga^{3+} is independent of the local structure of bulk Ga^{3+}, and that the former structure is the most important factor in the catalytic activity for CH_4-SCR.

3.3. UV–vis spectra of Ga_2O_3–Al_2O_3 catalysts treated with C_3H_6

The UV–vis spectra of C_3H_6-treated ST-dEtA(0.3), DGA(0.3) and CP(0.3) are shown in Fig. 3. When the catalysts pretreated in an O_2 atmosphere at 650 °C were exposed to C_3H_6 at 300 °C, they showed a sharp absorption band at ~340 nm and a broad absorption band at ~430 nm as a shoulder of the former band. These two absorption bands will be referred to as α and β bands, respectively. The band intensity relative to the O^{2-}-to-M^{3+} charge transfer band and the (α band)/(β band) area ratio varied greatly for the catalysts prepared by different methods. The α band intensity of ST-dEtA(0.3) which shows the highest activity for CH_4-SCR was the largest among the three catalysts, and the order of the α band intensity correlated with the catalytic activity for CH_4-SCR.

Similarly, UV–vis spectra were measured for a series of ST-dEtA(x) catalysts with various Ga/(Ga + Al) charged ratios, x (Fig. 4). Single component γ-Al_2O_3 (i.e., ST-dEtA(0)) exhibited neither the α band nor the β band. In contrast, the two bands were observed in the spectra of all of the other Ga^{3+}-containing catalysts. Therefore, the absorption bands observed when γ-Ga_2O_3–Al_2O_3 catalysts were allowed to react with C_3H_6 at 300 °C are

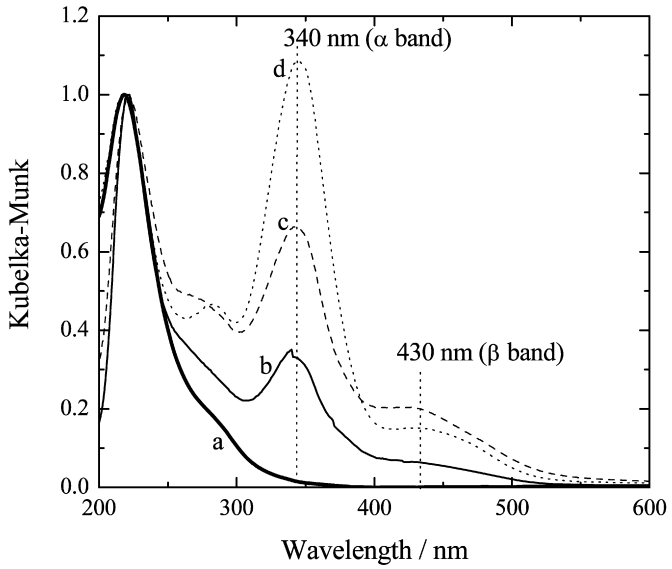

Fig. 3. UV–vis spectra of C_3H_6-treated Ga_2O_3–Al_2O_3 solid solutions. (a) ST-dEtA(0.3) without C_3H_6 treatment; (b) CP(0.3); (c) ST-DGA(0.3); (d) ST-dEtA(0.3).

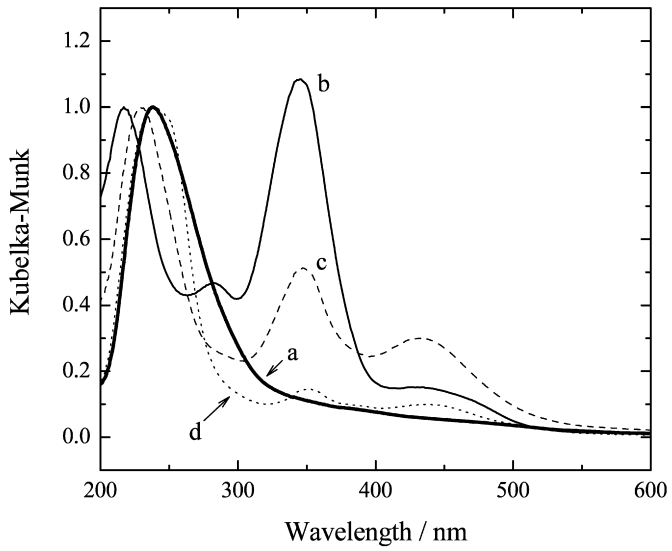

Fig. 4. UV–vis spectra of C_3H_6-treated ST-dEtA(x) catalysts: (a) ST-dEtA(0); (b) ST-dEtA(0.3); (c) ST-dEtA(0.75); (d) ST-dEtA(1.0).

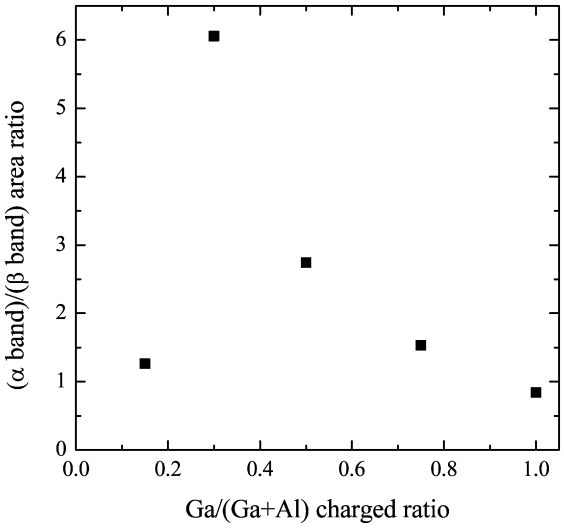

Fig. 5. Peak area ratio of (α band)/(β band) as a function of Ga/(Ga + Al) charged ratio.

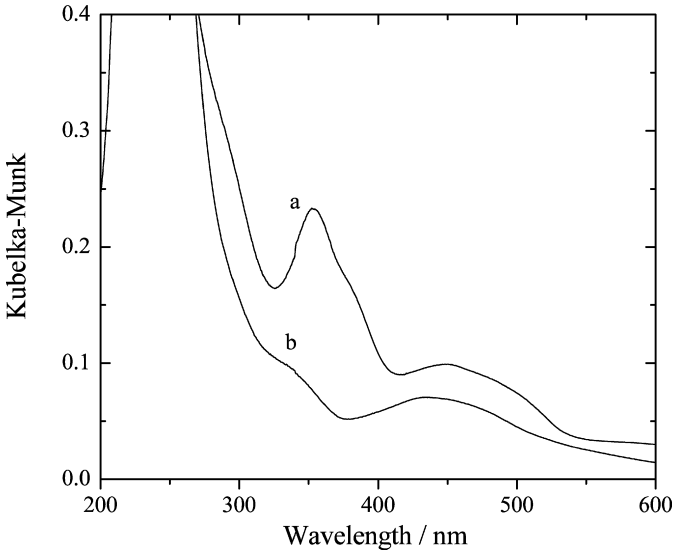

Fig. 6. UV–vis spectra of C_3H_6-teated $MgGa_2O_4$ (a) and $ZnGa_2O_4$ (b).

closely related to the interaction between Ga^{3+} and C_3H_6. The C_3H_6-treated ST-dEtA(0.3) catalyst exhibited the largest α band area, which decreased gradually as the Ga/(Ga+Al) ratio increased. On the other hand, the β band area of the C_3H_6-treated ST-dEtA(x) catalyst increased with an increase of x up to 0.75. The C_3H_6-treated γ-Ga_2O_3 catalyst (ST-dEtA(1.0)) showed both the α and β bands but the band areas were, however, much smaller than those of the Ga_2O_3–Al_2O_3 mixed oxides. Therefore, the interaction of Ga^{3+} and Al^{3+} (Ga–O–Al) was an important factor in exhibiting strong absorption bands in the C_3H_6-treated catalysts.

Ga^{3+} ions prefer to be located in the T_d sites of a spinel structure. This was confirmed by NMR spectra [9,17], and XAFS spectra as shown in this paper. Normal spinels belong to the space group *Fd3m*. There are 8 formula units per cubic unit cell. The anion sublattice of ideal spinel is arranged in cubic close-packed (*ccp*) spatial arrangement. There are 96 interstices between the anions in the cubic unit cell. Of the 64 tetrahedral interstices that exist between the anions, 8 are occupied by cations. The coordinates of the anions at equipoint 32e are not special: they vary according to a single parameter, u. For a perfect *ccp* anion arrangement, $u = 0.375$. As u increases from its ideal value, anions move away from the tetrahedrally coordinated A-site cations along the ⟨111⟩ directions, which increases the volume of each A-site interstice while the octahedral B-sites become correspondingly smaller [18].

Therefore, spinel structure can accommodate large Ga^{3+} ions in the T_d sites of the spinel structure. The amount of T_d-Ga^{3+} per gram of the catalyst increases with the increase in the Ga/(Ga+Al) ratio until Ga/(Ga + Al) = 0.3, where almost all of the T_d sites (A sites) of the spinel structure are occupied by Ga^{3+}. Further increase of the Ga/(Ga + Al) ratio results in an increase of the proportion of O_h-Ga^{3+}. In the UV–vis spectra of C_3H_6-treated ST-dEtA(x), the (α band)/(β band) area ratio of ST-dEtA(x) catalysts showed a maximum at Ga/(Ga + Al) = 0.3 and gradually decreased with an increase in the Ga/(Ga + Al) charged ratio (Fig. 5). This behavior corresponds exactly with the (T_d-Ga^{3+})/(O_h-Ga^{3+}) ratio in the bulk of ST-dEtA(x). Therefore, it is concluded that α and β bands are attributed to the propylene species adsorbed on T_d-Ga^{3+} and O_h-Ga^{3+}, respectively.

The UV–vis spectra of C_3H_6-treated $ZnGa_2O_4$ and $MgGa_2O_4$ are shown in Fig. 6. The former is a normal spinel where all of the

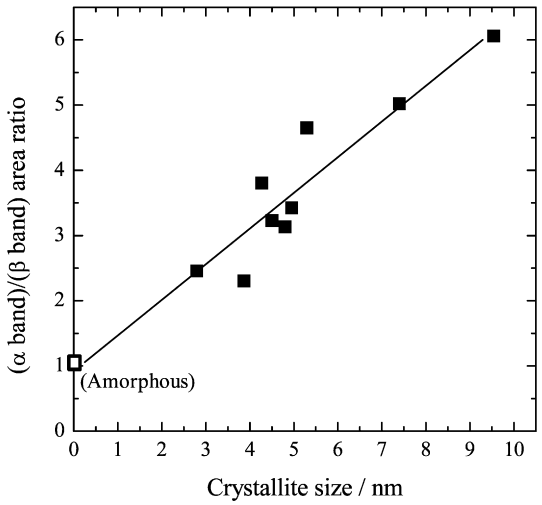

Fig. 7. Peak area ratio of (α band)/(β band) as a function of crystallite size (Table 2) of the Ga_2O_3–Al_2O_3 solid solutions.

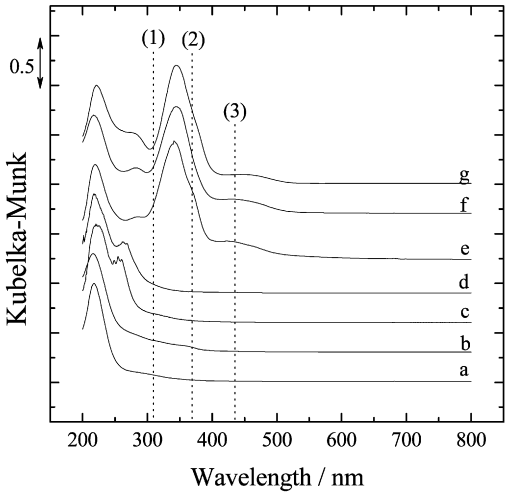

Fig. 8. UV–vis spectra of ST-dEtA(0.3) treated at 300 °C for 15 min with: (a) H_2 (30 Torr); (b) CH_4 (30 Torr); (c) benzene (40 Torr); (d) toluene (20 Torr); (e) C_2H_4 (30 Torr); (f) C_3H_6 (30 Torr); (g) *iso*-C_4H_8 (30 Torr). Wavelengths corresponding to monoenyl (1), dienyl (2), and trienyl (3) carbenium ions reported by Pazè et al. [20] are shown by the dotted lines.

Ga^{3+} ions occupy the O_h sites [16]. The latter is a disordered spinel where the proportion of (T_d-Ga^{3+})/(O_h-Ga^{3+}) can be varied from 0.5 to 1.0 [19]. These two gallium mixed oxides were selected as standard materials for O_h-Ga^{3+} and a mixture of T_d- and O_h-Ga^{3+}, respectively. In the case of C_3H_6-treated $ZnGa_2O_4$, a β band appeared in the UV–vis spectrum, but an α band was barely found at a shoulder of the O^{2-}-to-M^{3+} charge transfer band. On the other hand, the UV–vis spectrum of C_3H_6-treated $MgGa_2O_4$ exhibited α and β bands that were both intense. These results further support our conclusion that α and β bands are due to T_d-Ga^{3+} and O_h-Ga^{3+}, respectively.

The (α band)/(β band) area ratios of C_3H_6-treated Ga_2O_3–Al_2O_3 catalysts increased monotonically with their crystallite size as shown in Fig. 7. It has already been stated in Section 3.2 that the crystallite size of the solvothermally-prepared Ga_2O_3–Al_2O_3 solid solution hardly affected the local structure of Ga^{3+} in the bulk. However, the results shown in Fig. 7 suggest that the crystallite size of the catalyst influences the local structure of Ga^{3+} in the surface. Since the number of cations present on the surface of the catalyst is much lower than that present in the whole catalyst particle, the XAFS spectra of the Ga K-edge rather reflect the local structure of Ga^{3+} in the core of the crystals, which are essentially identical for all the catalysts as far as they have the same Ga/(Ga + Al) ratio (0.3) as shown in Table 2. If one supposes that the crystal shape is cubic and that (100), (010), and (001) planes are exposed, the proportion of cations existing in the outermost surface was calculated to be 6.7% for the 2.4-nm cubic crystal (3 × 3 × 3 unit cells) and 0.46% for the 9.6-nm cubic crystal (12 × 12 × 12 unit cells). The UV–vis bands observed in the spectrum of the C_3H_6-treated Ga_2O_3–Al_2O_3 catalyst come from adsorbed species and the spectrum reflects therefore the local structure of Ga^{3+} at the outermost layer of the surface of the catalyst particles.

3.4. UV–vis spectra of Ga_2O_3–Al_2O_3 treated with various adsorbates

The UV–vis spectra of ST-dEtA(0.3) heated at 300 °C in various adsorbates are shown in Fig. 8. When aliphatic alkenes such as ethylene, 1-butene and isobutene were introduced to the catalyst, a strong α band appeared in the UV–vis spectra together with a weak β band. The wavelengths of both bands are almost the same within analytical error indicating that the same adsorbed species was formed on the Ga_2O_3–Al_2O_3 surface irrespective of whether alkenes had alkyl side-chains or not. On the other hand, no absorption band appeared when H_2 and CH_4 were introduced to

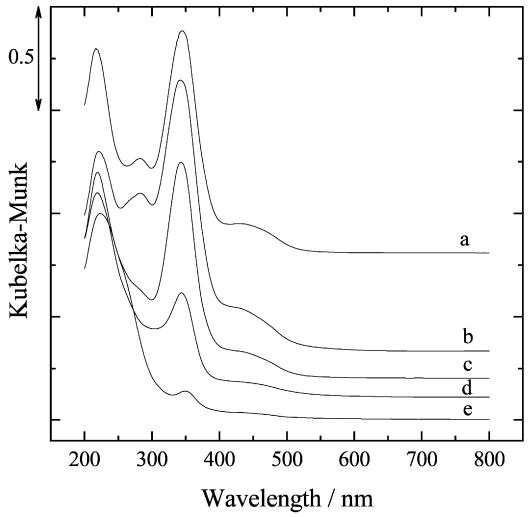

Fig. 9. UV–vis spectra of C_3H_6-treated ST-dEtA(0.3) (spectrum (a)) with subsequent treatment with: (b) H_2 (30 Torr); (c) O_2 (30 Torr); (d) H_2O (18 Torr × 1); (e) H_2O (18 Torr × 2).

the catalysts, although the pressure of these two adsorbates (H_2 and CH_4) decreased during heating the catalyst up to 300 °C, indicating that adsorption of these two species on the catalyst did occur. There were no absorption bands in the 340–500-nm range when the catalyst was treated with aromatic compounds (benzene and toluene). These results indicate that the surface Ga^{3+} reacted with aliphatic alkenes to give α and β bands in the UV–vis spectra. Moreover, Ga^{3+} in γ-Ga_2O_3–Al_2O_3 could discriminate between aliphatic alkenes and aromatic compounds.

Fig. 9 shows the change of the UV–vis spectra by the subsequent treatments of adsorbed species. The α and β bands in the UV–vis spectrum of C_3H_6-treated ST-dEtA(0.3) remained unchanged after evacuation at room temperature, indicating that the adsorbed species were not eliminated under vacuum. Even when O_2, or H_2 was introduced to C_3H_6-treated ST-dEtA(0.3) at room temperature, these bands were also maintained. However, the α and β bands disappeared when water was introduced to C_3H_6-treated ST-dEtA(0.3).

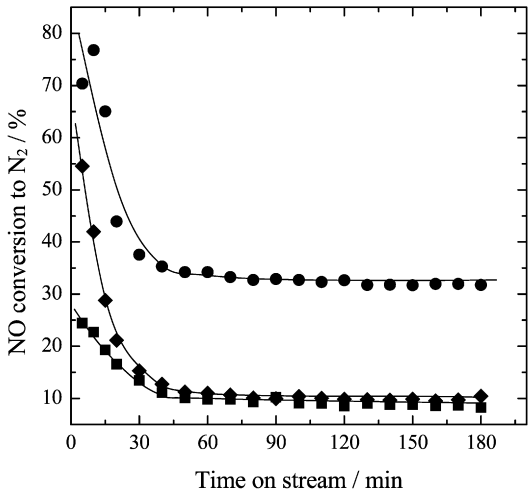

Fig. 10. Initial and steady-state activities of the Ga_2O_3–Al_2O_3 catalysts: (●) ST-dEtA(0.3); (◆) ST-DGA(0.3); (■) CP(0.3). Reaction conditions: NO 1000 ppm, CH_4 2000 ppm, O_2 6.7%, He balance.

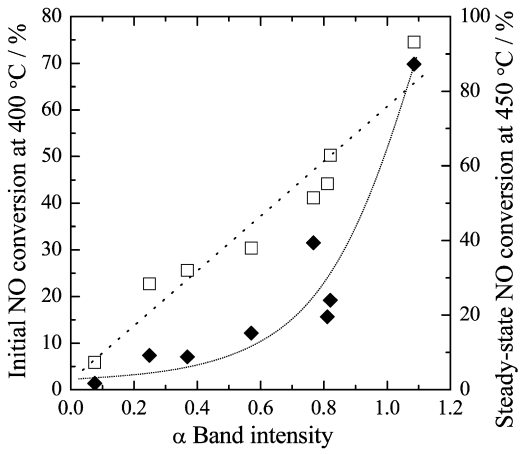

Fig. 11. Initial (□) and steady-state NO conversions (◆) over the Ga_2O_3–Al_2O_3 catalysts as a function of the α band intensity of their UV–vis spectra after C_3H_6 treatment. Initial activity was determined under the condition of 400 °C, NO 1000 ppm, CH_4 2000 ppm, O_2 6.7% and He balance, while steady-state activity was determined: 450 °C, NO 1000 ppm, CH_4 1000 ppm, O_2 6.7% and He balance.

There are many research articles on the interaction between alkenes and solid acids [20]. Demidov and Davydov reported absorption bands at 300–450 nm in the UV–vis spectrum of alkene-treated H-ZSM-5 [21]. Pazè et al. examined the UV–vis spectrum of 1-butene-treated H-ferrierite zeolite [22]. They both assigned the high-wavelength bands as π–π^* transition of carbenium ions adsorbed on the acid sites of the zeolites: 290–310-, 350–380-, and 430–450-nm bands were assigned to monoenyl (allyl), dienyl, and trienyl cations respectively. With increasing temperature, the absorption band due to monoenyl carbenium ions diminished which is associated with the appearance of new bands due to dienyl and trienyl carbenium ions. It was also reported that the carbenium ions formed on the metal oxides were easily desorbed by the addition of H_2O, or NH_3, resulting in the disappearance of these bands [23,24].

Since the wavelengths of the absorption bands observed for C_3H_6-treated ST-dEtA(0.3) were near to those reported for alkene–zeolite systems, together with similar behavior against water, it may be assumed that similar carbenium ions are the origin of the α and β bands observed in the C_3H_6-treated catalyst. However, no new bands other than α and β bands for C_3H_6-treated ST-dEtA(0.3) appeared with increasing temperature, although the (α band)/(β band) area ratio was changed presumably because of the collapse of the carbenium ion adsorbed on Ga^{3+}. Moreover, the difference in the wavelengths between the α and β bands is about 90 nm, significantly larger than that between the absorption bands due to monoenyl and dienyl carbenium ions. Therefore, the idea that carbenium ions having expanded conjugation systems (dienyl and trienyl carbenium ions) give an absorption band at ~430 nm cannot be accepted in the present case, and α and β bands must be due to the carbenium ion interacting with T_d- and O_h-Ga^{3+} ions.

3.5. Evaluation of catalytic activity of Ga_2O_3–Al_2O_3 using C_3H_6 as a probe

The initial activities of the catalysts were examined, and the results are shown in Fig. 10. The catalyst, ST-dEtA(0.3), converted 78% NO at the initial stage of the reaction, but its activity gradually decreased with time on stream. The NO conversion of each catalyst reached steady state within 40 min. Although the steady-state activities of ST-DGA(0.3) and CP(0.3) were the same, the initial activity of ST-DGA(0.3) was two times higher than that of CP(0.3). Because the initial activities of the catalysts varied greatly, the adsorption-desorption behavior of water on the catalyst surface [14] was not the sole factor determining the performance of the Ga_2O_3–Al_2O_3 catalysts.

As mentioned above, the intensities of the α and β bands were closely related with the catalytic activity of Ga_2O_3–Al_2O_3 (Ga/(Ga + Al) = 0.3) (Fig. 3). Therefore, correlation between activity of the catalyst for CH_4-SCR and the intensities of the α and β bands of the C_3H_6-treated catalyst were examined. Fig. 11 shows that the initial NO conversion of the catalyst with a Ga/(Ga + Al) ratio of 0.3 increases linearly with an increase in the intensity of the α band. In the Ga_2O_3–Al_2O_3 system, the steady-state activity for the CH_4-SCR reaction was significantly affected by water produced by the reaction [7,10]. In the initial stage of the reaction, the surface of the catalyst is free from adsorbed water and all of the active sites can be considered to have ability for the reduction of NO with CH_4. Then, the initial activity of the catalysts is thought to represent the number of active sites of the Ga_2O_3–Al_2O_3 catalyst. The fact that the initial activity of the catalyst increases linearly with α band intensity suggests that the surface T_d-Ga^{3+} is the active site for the CH_4-SCR reaction. Since the intensity of α and β bands became stronger when Ga^{3+} and Al^{3+} co-existed in the catalyst, the interaction of Ga^{3+} with Al^{3+} seems to be an important factor in giving an intense α band. Because of the inhibitory effect of water produced by the reaction, the steady-state NO conversion of the catalyst correlates roughly with α band intensity: The catalyst showing a more intense α band in the UV–vis spectrum of the C_3H_6-treated sample is more active for the CH_4-SCR reaction.

Fig. 12 shows the steady-state activity of the catalyst with the Ga/(Ga + Al) charged ratio of 0.3 plotted against the (α band)/(β band) area ratio in the UV–vis spectrum of the C_3H_6-treated γ-Ga_2O_3–Al_2O_3 catalyst. In our previous research, we showed that the steady-state activities of γ-Ga_2O_3–Al_2O_3 catalysts for CH_4-SCR were in proportion with their crystallite sizes. The (α band)/(β band) area ratios in the UV–vis spectra of the C_3H_6-treated γ-Ga_2O_3–Al_2O_3 catalysts showed proportional correlation with their crystallite sizes. Therefore, propylene can be used as a probe to evaluate not only the amount of surface active sites but also the steady-state activity of γ-Ga_2O_3–Al_2O_3 catalysts with the same Ga/(Ga + Al) composition.

4. Conclusions

Two absorption bands at 340 nm (α band) and 430 nm (β band) were observed in the UV–vis spectra of C_3H_6-treated γ-

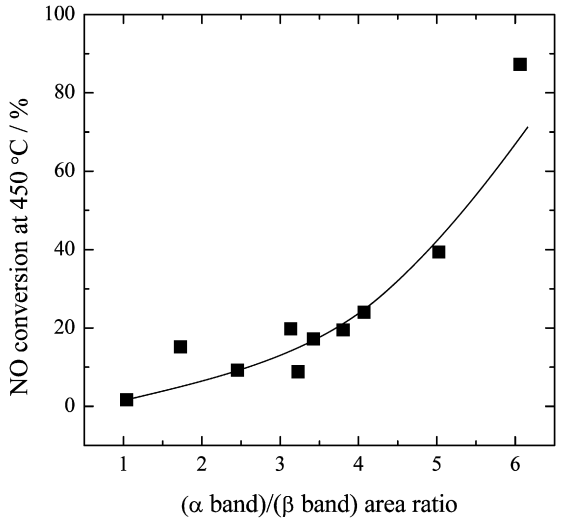

Fig. 12. Steady-state NO conversion over the Ga_2O_3–Al_2O_3 catalysts as a function of the (α band)/(β band) area ratio of their UV–vis spectra after C_3H_6-treatment. Reaction conditions: 450 °C, NO 1000 ppm, CH_4 2000 ppm, O_2 6.7%, He balance.

Ga_2O_3–Al_2O_3 solid solutions. The α and β bands were assigned to carbenium ions adsorbed on T_d-Ga^{3+} and O_h-Ga^{3+}, respectively.

The intensity of the α band represented the number of active sites on the γ-Ga_2O_3–Al_2O_3 catalyst surface quantitatively. The steady-state activity of the γ-Ga_2O_3–Al_2O_3 catalyst with the same composition was also evaluated by the UV–vis spectrum of the C_3H_6-treated sample. An effective parameter for distinguishing between activities of catalysts with the same Ga/(Ga + Al) ratio was provided by the use of a C_3H_6 molecule as a probe. The UV–vis spectrum of the C_3H_6-treated Ga_2O_3–Al_2O_3 catalyst is very sensitive to the environment of the surface Ga^{3+} ion and is a useful tool for analysis of active species of surface Ga^{3+}.

This paper showed that the structure in the outermost surface of oxide particles is different from that of the bulk crystal, and an analytical method to evaluate the local structure of Ga^{3+} ions in the outermost surface of Ga-containing oxide catalysts using C_3H_6 as a probe was suggested.

Acknowledgment

The XAFS experiments were performed at BL16B2 in SPring-8 with the approval of the Japan Synchrotron Radiation Research Institute (JASRI) (proposal No. C05A16B2-4050-N).

References

[1] Z. Liu, S.I. Woo, Catal. Rev.-Sci. Eng. 48 (2006) 43.
[2] M.C. Campa, D. Pietrogiacomi, S. Tuti, G. Ferraris, V. Indovina, Appl. Catal. B 18 (1998) 151.
[3] C. Resini, T. Montanari, L. Nappi, G. Bagnasco, M. Turco, G. Busca, F. Bregani, M. Notaro, G. Rocchini, J. Catal. 214 (2003) 179.
[4] J.-H. Park, C.H. Park, I.-S. Nam, Appl. Catal. A 277 (2004) 271.
[5] K. Yogo, M. Ihara, I. Terasaki, E. Kikuchi, Chem. Lett. 22 (1993) 229.
[6] X. Zhou, T. Zhang, Z. Xu, L. Lin, Catal. Lett. 40 (1996) 35.
[7] K. Shimizu, A. Satsuma, T. Hattori, Appl. Catal. B 16 (1998) 319.
[8] K. Shimizu, M. Takamatsu, K. Nishi, H. Yoshida, A. Satsuma, T. Tanaka, S. Yoshida, T. Hattori, J. Phys. Chem. B 103 (1999) 1542.
[9] M. Takahashi, N. Inoue, T. Takeguchi, S. Iwamoto, M. Inoue, J. Am. Ceram. Soc. 89 (2006) 2158.
[10] M. Takahashi, N. Inoue, T. Nakatani, T. Takeguchi, S. Iwamoto, T. Watanabe, M. Inoue, Appl. Catal. B 65 (2006) 142.
[11] M. Takahashi, T. Nakatani, S. Iwamoto, T. Watanabe, M. Inoue, J. Phys. Condens. Matter 18 (2006) 5745.
[12] M. Haneda, Y. Kintaichi, H. Shimada, H. Hamada, J. Catal. 192 (2000) 137.
[13] M. Takahashi, T. Nakatani, S. Iwamoto, T. Watanabe, M. Inoue, Appl. Catal. B 70 (2007) 73.
[14] M. Takahashi, T. Nakatani, S. Iwamoto, T. Watanabe, M. Inoue, Ind. Eng. Chem. Res. 45 (2006) 3678.
[15] M. Inoue, J. Phys. Condens. Matter 16 (2004) S1291.
[16] R.J. Hill, J.R. Graig, G.V. Gibbs, Phys. Chem. Miner. 4 (1979) 317.
[17] C. Otero Areán, M. Rodríguez Delgado, V. Montouillout, D. Mossiot, Z. Anog. Allg. Chem. 631 (2005) 2121.
[18] K.E. Sickafus, J.M. Wills, N.M. Grimes, J. Am. Ceram. Soc. 82 (1999) 3279.
[19] J.E. Weidenborner, N.R. Stemple, Y. Okaya, Acta Crystallogr. 20 (1966) 761.
[20] I. Kiricsi, H. Förster, G. Tasi, J.B. Nagy, Chem. Rev. 99 (1999) 2085.
[21] A.V. Demidov, A.A. Davydov, Mater. Chem. Phys. 39 (1994) 13.
[22] C. Pazè, B. Sazak, A. Zecchina, J. Dwyer, J. Phys. Chem. B 103 (1999) 9978.
[23] H.P. Leftin, W.K. Hall, J. Phys. Chem. 66 (1962) 1457.
[24] S. Bordiga, G. Ricchiardi, G. Spoto, D. Scarano, L. Carnelli, A. Zecchina, C.O. Arean, J. Chem. Soc. Faraday Trans. 89 (1993) 1843.